J Fluoresc (2008) 18:109–118
DOI 10.1007/s10895-007-0247-4

ORIGINAL PAPER

Fluorescence Study on the Interaction of Bovine Serum Albumin with P-Aminoazobenzene

Ye-Zhong Zhang · Bo Zhou · Yan-Xia Liu · Chun-Xia Zhou · Xin-Liang Ding · Yi Liu

Received: 9 July 2007 / Accepted: 17 August 2007 / Published online: 25 September 2007
© Springer Science + Business Media, LLC 2007

Abstract In this paper, the interaction between p-aminoazobenzene (PAAB) and BSA was investigated mainly by fluorescence quenching spectra, circular dichroism (CD) and three-dimensional fluorescence spectra under simulative physiological conditions. It was proved that the fluorescence quenching of BSA by PAAB was mainly a result of the formation of a PAAB-BSA complex. The modified Stern-Volmer quenching constant K_a and the corresponding thermodynamic parameters ΔH, ΔG and ΔS at different temperatures were calculated. The results indicated that van der Waals interactions and hydrogen bonds were the predominant intermolecular forces in stabilizing the complex. The distance r=4.33 nm between the donor (BSA) and acceptor (PAAB) was obtained according to Förster's non-radioactive energy transfer theory. The synchronous fluorescence, CD and three-dimensional fluorescence spectral results showed that the hydrophobicity of amino acid residues increased and the losing of α-helix content (from 63.57 to 51.83%) in the presence of PAAB. These revealed that the microenvironment and conformation of BSA were changed in the binding reaction.

Y.-Z. Zhang · Y.-X. Liu · C.-X. Zhou · Y. Liu (✉)
Department of Chemistry, College of Chemistry and Environmental Engineering, Yangtze University, JingZhou, Hubei 434025, People's Republic of China
e-mail: prof.liuyi@263.net

Y.-Z. Zhang · B. Zhou · X.-L. Ding · Y. Liu
Department of Chemistry, College of Chemistry and Molecular Sciences, Wuhan University, Wuhan, Hubei 430072, People's Republic of China

Keywords P-aminoazobenzene · Bovine serum albumin · Fluorescence quenching · Circular dichroism · Three-dimensional fluorescence spectra

Introduction

Serum albumin as one of the most abundant carrier proteins plays an important role in the transport and disposition of endogenous and exogenous compounds present in blood. Distribution and metabolism of many biologically active compounds such as metabolites, drugs and other organic compounds in the body are correlated with their affinities towards serum albumin, and the binding ability of drugs-albumin in blood stream may have a significant impact on free concentration and metabolism of drugs [1, 2]. Strong binding can decrease the concentrations of free drugs in plasma, whereas weak binding can lead to a short lifetime or poor distribution. Consequently, the investigation of the binding between drugs and serum albumin is of fundamental importance in pharmacology and pharmacodynamics. Therefore, the binding of drugs to serum albumin in vitro, considered as a model in protein chemistry to study the binding behavior of proteins, has been an interesting research field in chemistry, life sciences and clinical medicine and has been studied for many years [3–6]. In this work, bovine serum albumin (BSA) was selected as our protein model because of its low cost, ready availability, unusual ligand-binding properties, and the results of all the studies are consistent with the fact that bovine and human serum albumins are homologous proteins [7–9].

Azobenzene is a kind of azo dyes and its derivatives have been found extensive applicability in areas such as dyestuffs, pH indicators, nonlinear optical chromophores, photostorage units, and triggers for optical switching [10–

14]. Currently azo dyes have been extensively used in the printing and dyeing for textile, leather, paper and food, etc. It should be noted that at the normal circumstances, azo dyes would not be harmful to the human body. While some of those dyes synthesized by using the carcinogenic aromatic amine, after the long-term contact with human skin, can combine and react with the materials released by the normal metabolic process and then induced the fracture of the N=N structure and the newly formation of the carcinogenic aromatic compounds. These newly formed compounds were then absorbed again by human body and result in the structure and function of human cell changed, which result in the increasing possibility of the occurrence of cancer. P-aminoazobenzene (PAAB, see Fig. 1) is a sort of the carcinogenic aromatic amine which is commonly used as the intermediates of azo dyes. And it has been recommended as a unsafe substance because it may cause cancer to people. So it is necessary for us to carry out detailed investigation of the binding affinities of PAAB to protein. And in this paper BSA was selected as the protein model for the reasons mentioned above. We hope this work cannot only provide useful information for appropriately understanding the toxicological action of active components in dyes, but also illustrate its binding affinity and binding mechanisms at a molecular level.

As BSA has two tryptophan residues that possess intrinsic fluorescence: Trp-212, located within a hydrophobic binding pocket in the subdomain IIA, and Trp-134, located on the surface of the albumin molecule in the first subdomain IB [15]. Therefore, fluorescence technique can be considered as a feasible and powerful tool for the measurements. In this paper, the interaction between PAAB and BSA was studied under physiological conditions mainly by fluorescence quenching spectra, circular dichroism and three-dimensional fluorescence spectra. Great attempts were made to investigate the binding mechanism between PAAB and BSA regarding the binding constants, the thermodynamic parameters and the effect of PAAB on the conformation of BSA. In addition, three-dimensional fluorescence spectra is a newly developed fluorescence analytical technique which can comprehensively exhibit the fluorescence information of the sample, making the investigation of the characteristic conformational change of protein be more scientific and credible. In the previous drug-protein investigations, this method was few used and the interpretation of the fluorescence information was incomprehensive. So we made a detailed and insightful analysis of the fluorescence information exhibited by this spectrum in the present work.

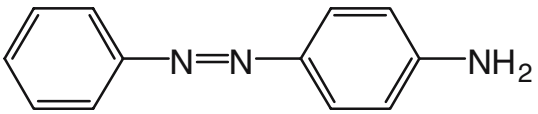

Fig. 1 Structure of PAAB

Experimental

Materials

BSA was purchased from Sigma, PAAB was purchased from the third reagent Co., Ltd (Shanghai, China). All BSA solution was prepared in the Tris-HCl buffer solution (0.05 mol l^{-1} tris, 0.15 mol l^{-1} NaCl, pH 7.4). NaCl, HCl, and other chemicals were all of analytical purity. And the PAAB solution was prepared in ethanol. Doubly distilled water was used throughout the experiment. The weight measurements were performed with an AY-120 electronic analytic weighting scale (Shimadzu, Japan) with a resolution of 0.1 mg.

Fluorescence and UV–vis absorbance spectra

Fluorescence spectra were recorded on a LS-55 Spectrofluorimeter (Perkin-Elmer corporate, America) equipped with 1.0 cm quartz cells and a thermostat bath. Fluorescence spectra were recorded at 292, 298, 304, 310 *K* in the range of 300–460 nm. The width of the excitation and emission slit was set to 15.0 and 4.0 nm, respectively. An excitation wavelength of 285 nm was chosen and very dilute solutions were used in the experiment (BSA 2.0×10^{-6} mol l^{-1}, PAAB in the range of $0–7.0\times10^{-6}$ mol l^{-1}) to avoid inner filter effect. The quenching effect of ethanol was evaluated and the result indicated that there was almost no affection of ethanol on the PAAB-BSA interaction.

The three-dimensional fluorescence spectra were performed under the following conditions: the emission wavelength was recorded between 200 and 500 nm, the initial excitation wavelength was set to 200 nm with increment of 5 nm, the number of scanning curves was 31, and other scanning parameters were just the same to that of the fluorescence quenching spectra.

The UV-vis spectra were recorded at room temperature on a TU-1901 spectrophotometer (Puxi Analytic Instrument Ltd. of Beijing, China) equipped with 1.0 cm quartz cells. The range of wavelength was from 340 to 200 nm.

Circular dichroism measurements

Circular dichroism (CD) spectra were measured by a J-810 Spectropolarimeter (Jasco, Tokyo, Japan) at room temperature under constant nitrogen flush. Quartz cells have path length and volume of 0.1 cm and 400 μl, respectively. The scanning speed was set to 200 nm/min. The CD measurements of BSA in the absence and presence of PAAB (1:2,

1:6, 1:10) were made in the range of 200–260 nm. The CD results were expressed in terms of mean residue ellipticity (MRE) in deg cm^2 $dmol^{-1}$. Appropriate blanks, run under the same conditions, were subtracted from the sample spectra.

Results and discussions

Effect of PAAB on BSA fluorescence

Fluorescence quenching refers to any process which decreases the fluorescence intensity of a sample such as excited state reactions, energy transfers, ground-state complexes formation and collisional process [16]. BSA has three intrinsic fluorophores: tryptophan, tyrosine and phenylalanine that can be quenched. In fact, as Sulkowska [17] said, because phenylalanine has a very low quantum yield and the fluorescence of tyrosine is almost totally quenched if it is ionized, or near an amino group, a carboxyl group, or a tryptophan, the intrinsic fluorescence of BSA is almost contributed by tryptophan alone. Here PAAB is a quencher which can quench the fluorescence intensity of BSA when bond to BSA. We measured the fluorescence quenching spectra of BSA at various concentrations of PAAB under physiological condition.

From Fig. 2, we can see clearly that BSA had a strong fluorescence emission band at 350 nm by fixing the excitation wavelength at 285 nm, while PAAB had no intrinsic fluorescence. The fluorescence intensity of BSA decreased regularly and the maximum emission wavelength underwent an obvious blue shift of up to 7 nm (from 351 to 344 nm) with the increasing of PAAB concentration. The blue shift effect expressed that the conformation of BSA changed. It also indicated that the polarity around the tryptophan residues decreased and the hydrophobicity increased.

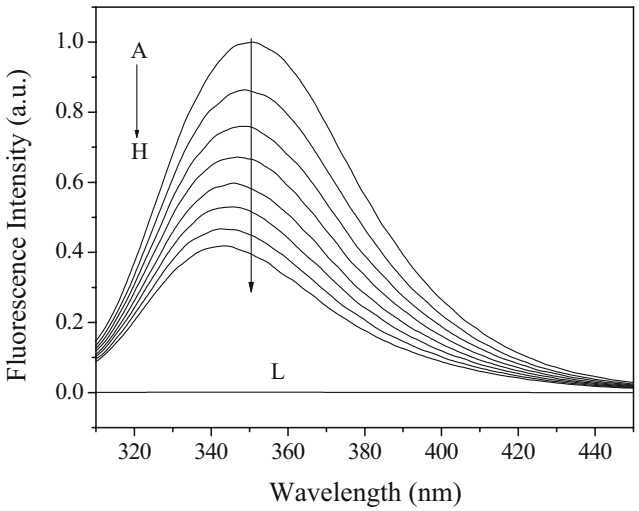

Fig. 2 Emission spectra of BSA in the presence of various concentrations of PAAB (T=298 K, λ_{ex}=285 nm). c(BSA)=2.0×10^{-6} mol l^{-1}; c(PAAB)/(10^{-6} mol l^{-1}), *A–H*: 0, 1.0, 2.0, 3.0, 4.0, 5.0, 6.0, 7.0, respectively; curve *L* shows the emission spectrum of PAAB only

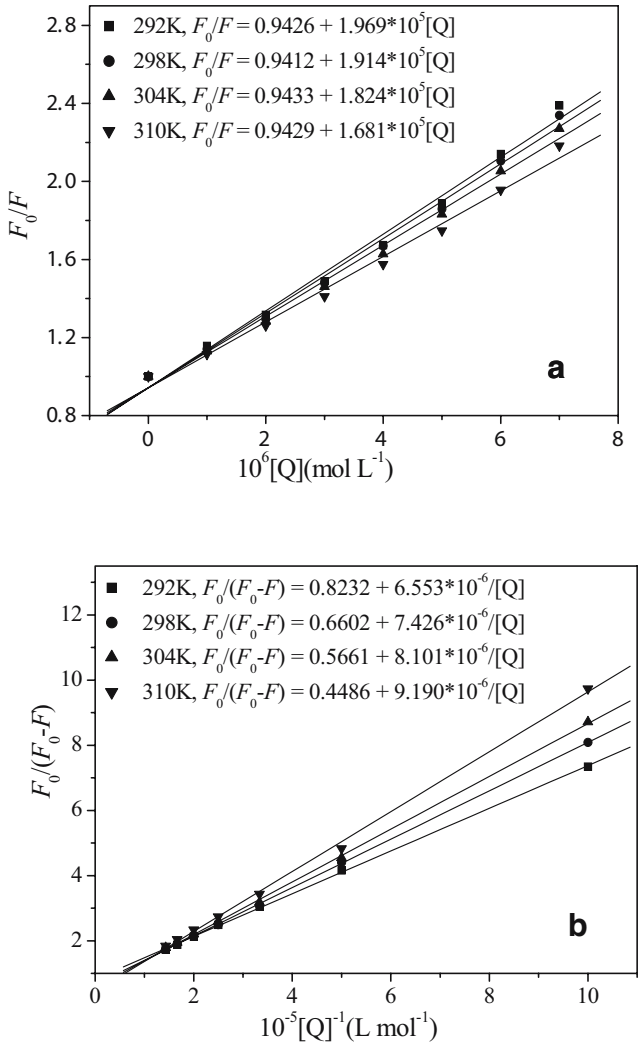

Fig. 3 Stern-Volmer plots (**a**) and modified Stern-Volmer plots (**b**) for the quenching of BSA by PAAB at four different temperatures

Table 1 Stern-Volmer quenching constants for the interaction of PAAB with BSA at different temperatures

pH	T (K)	K_{SV} ($\times10^5$ l mol^{-1})	k_q($\times10^{13}$L mol^{-1} s^{-1})	R^a	S.D.[b]
7.4	292	1.969	1.969	0.9952	0.051
	298	1.914	1.914	0.9960	0.045
	304	1.824	1.824	0.9964	0.041
	310	1.681	1.681	0.9951	0.044

[a] R is the correlation coefficient.
[b] S.D. is the standard deviation for the K_{SV} values.

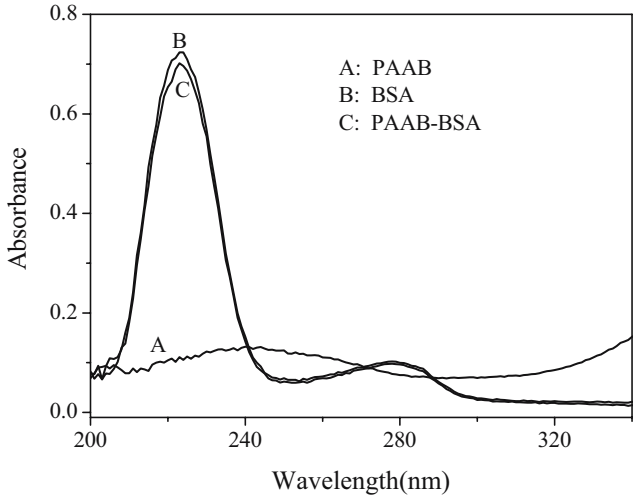

Fig. 4 The UV–vis spectra of BSA and PAAB; *A* indicates PAAB, *c* (PAAB)=2.0×10^{-6} mol l^{-1} (buffer solution as reference); *B* indicates BSA, *c*(BSA)=2.0×10^{-6} mol l^{-1} (buffer solution as reference); *C* indicates PAAB-BSA, *c*(PAAB)=*c*(BSA)=2.0×10^{-6} mol l^{-1} (1:1) (PAAB as reference)

The fluorescence quenching mechanism

The different mechanisms of quenching are usually classified as dynamic quenching and static quenching. Dynamic and static quenching can be distinguished by their differing dependence on temperature and viscosity. Since higher temperature result in larger diffusion coefficients, the dynamic quenching constants are expected to increase with increasing temperature. In contrast, increased temperature is likely to result in decreased stability of complexes, and thus lower values of the static quenching constants [18].

For dynamic quenching, the fluorescence data at different temperatures were analyzed by the well-known Stern-Volmer equation [19, 20]:

$$\frac{F_0}{F} = 1 + K_{SV}[Q] = 1 + k_q\tau_0[Q] \quad (1)$$

where F_0 and F denote the steady-state fluorescence intensities in the absence and presence of quencher (PAAB), respectively. K_{SV} is the Stern-Volmer quenching constant, and [Q] is the concentration of PAAB. k_q is the quenching rate constant of the biological macromolecule. The Stern-Volmer plots are shown in Fig. 3a. Accordingly, Eq. 1 was applied to determine K_{SV} by linear regression of a plot of F_0/F against [Q]. τ_0 is the average lifetime of the molecule without any quencher and the fluorescence lifetime of the biopolymer is 10^{-8} s [21, 22].

In Table 1, the Stern-Volmer quenching constant K_{SV} is inversely correlated with temperature and k_q is much greater than the value of the maximum scatter collision quenching constant (2.0×10^{10} l mol^{-1} s^{-1}, [23, 24]). The results indicated that the fluorescence quenching was caused by a specific interaction, and the quenching was mainly arisen by complex formation [25]. Moreover, the UV-vis absorption spectra of BSA, PAAB and the PAAB-BSA system (Fig. 4) were different obviously. This result confirmed that the quenching was mainly a static quenching process.

Consequently, the quenching data were analyzed according to the modified Stern-Volmer equation [26]:

$$\frac{F_0}{\Delta F} = \frac{1}{f_a K_a}\frac{1}{[Q]} + \frac{1}{f_a} \quad (2)$$

In the present case, ΔF is the difference of fluorescence intensity in absence and presence of the quencher at concentration [Q], f_a is the fraction of accessible fluorescence, and K_a is the effective quenching constant for the accessible fluorophores, which are analogous to associative binding constants for the quencher-acceptor system. The modified Stern-Volmer plots are shown in Fig. 3b, and the corresponding quenching constants K_a at four different temperatures are presented in Table 2.

The interaction force between PAAB and BSA

Generally speaking, small organic molecules are bound to biological macromolecules through four binding modes: hydrogen bond, van der Waals force, electrostatic interactions and hydrophobic interactions, etc. Ross [27] summed up the thermodynamic laws for estimating the type of the binding force between organic micro-molecule and biological macromolecule. That is, hydrophobic force may increase ΔH and ΔS of a system, while hydrogen bond and van der Waals force may decrease them, and electrostatic force usually makes $\Delta H\approx0$ and $\Delta S>0$. If the temperature changes a little, the enthalpy change can be

Table 2 Modified Stern-Volmer association constants K_a and relative thermodynamic parameters of the system of PAAB-BSA

T (K)	K_a($\times10^5$ l mol^{-1})	R^a	ΔH(kJ mol^{-1})	ΔG(kJ mol^{-1})	ΔS(J mol^{-1} K^{-1})	R^b
292	1.256	0.9998	−51.38	−28.50	−78.36	0.9884
298	0.889	0.9999		−28.23		
304	0.699	0.9997		−28.19		
310	0.488	0.9992		−27.82		

[a] *R* is the correlation coefficient for the K_a values.
[b] *R* is the correlation coefficient for the van't Hoff plot.

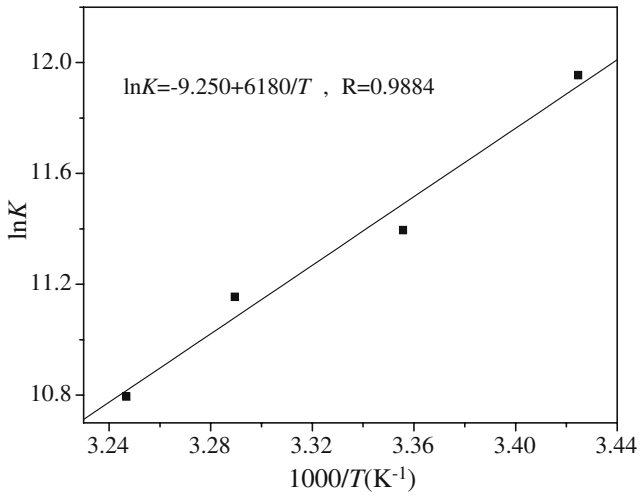

Fig. 5 Van't Hoff plot for the interaction of BSA and PAAB in tris-buffer, pH=7.4

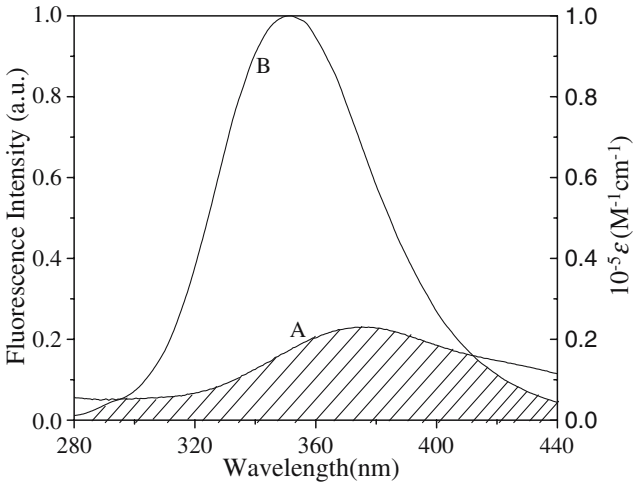

Fig. 6 Spectral overlaps of PAAB absorption (**a**) with BSA fluorescence (**b**) spectra. c(BSA)=c(PAAB)=2.0×10^{-6} mol l^{-1} (T= 298 K)

regarded as a constant. And the value of enthalpy change (ΔH) and entropy change (ΔS) can be estimated from the van' t Hoff equation [28]:

$$\ln K = -\frac{\Delta H}{RT} + \frac{\Delta S}{R} \tag{3}$$

where the associative binding constant K is analogous to the effective quenching constant K_a at the corresponding temperature (the temperatures used were 292, 298, 304, and 310 K), R is the gas constant. The temperature dependence of the binding constants was studied at the four different temperatures and the slope of a plot of the bimolecular quenching constant versus $1/T$ are linear within experimental error (Fig. 5), which allows one to calculate the energy change in the quenching process. The free energy change (ΔG) can be obtained from the following relationship:

$$\Delta G = \Delta H - T\Delta S = -RT\ln K \tag{4}$$

According to Eqs. 3 and 4, the values of ΔG, ΔH and ΔS were obtained and shown in Table 2. As can be seen from Table 2, the negative sign for free energy (ΔG) means that the interaction process is spontaneous. The negative ΔH (−51.38 kJ mol^{-1}) and negative ΔS (−78.36 J mol^{-1} K^{-1})

Table 3 Apparent binding constants K_b and binding sites n at different temperatures

pH	T (K)	K_b(×10^5 l mol^{-1})	n	R^a	S.D.[b]
7.4	292	1.265	1.169	0.9995	0.025
	298	1.085	1.158	0.9994	0.026
	304	0.837	1.140	0.9991	0.039
	310	0.592	1.118	0.9980	0.047

[a] R is the correlation coefficient.
[b] S.D. is the standard deviation for the K_b values.

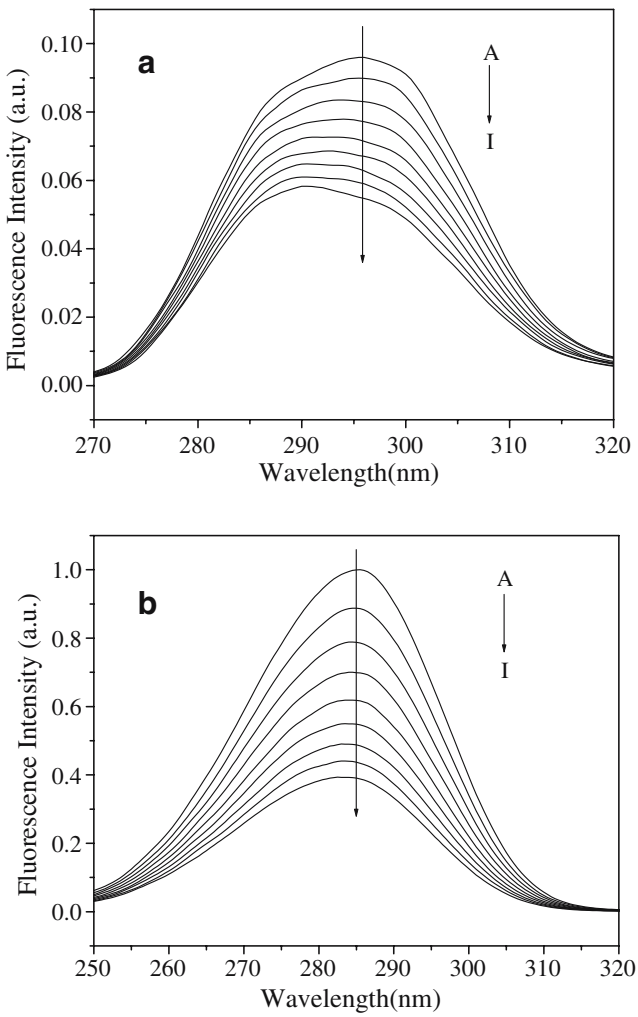

Fig. 7 Synchronous fluorescence spectra of BSA: **a** $\Delta\lambda$=15 nm; **b** $\Delta\lambda$=60 nm. c(BSA)=2.0×10^{-6} mol l^{-1}; c(PAAB)/(10^{-6} mol l^{-1}) A–H: 0, 1.0, 2.0, 3.0, 4.0, 5.0, 6.0, 7.0, respectively

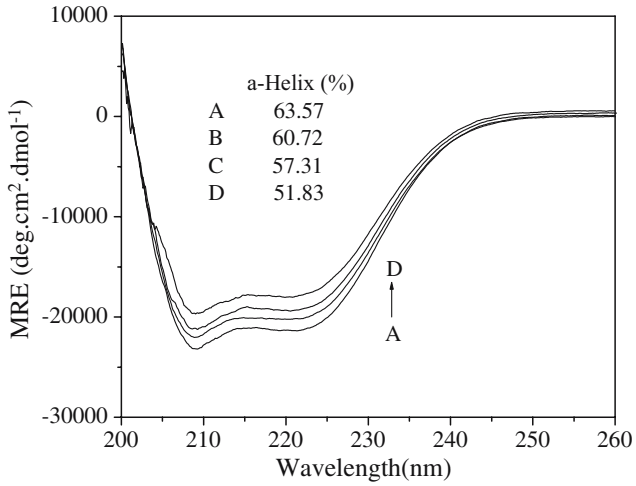

Fig. 8 CD spectra of the PAAB-BSA system at pH=7.4. c(BSA)=2.0×10^{-6} mol l^{-1}, c(PAAB)/(10^{-5} mol l^{-1}) *A–D*: 0, 0.4, 1.2, 2.0, respectively

indicated that hydrogen bonds and van der Waals force played major roles in the acting force and the reaction was mainly enthalpy-driven [27].

Numbers of binding sites and binding locality

For static quenching, the following equation was employed to calculate the binding constant and binding sites [29, 30].

$$\log\frac{F_0-F}{F}=\log K_b+n\log[Q] \tag{5}$$

where F_0 and F are the fluorescence intensities of BSA in the absence and presence of quencher (PAAB), K_b and n are the binding constant and binding sites, respectively. The dependence of log ($F_0/F-1$) on the value of log[Q] is linear with slope equal to the value of n and the value of logK_b is fixed on the ordinate. Table 3 shows the values of K_b and n, and it can be seen that K_b decreased with the rising of temperature which may indicate the forming of an unstable PAAB-BSA complex in the binding reaction. The complex would possibly be partly decomposed when the temperature increases. Therefore, the values of K_b and n decreased with the rising temperatures, which was in accordance with the trend of K_a as mentioned above.

The distance r between the donor and acceptor can be calculated according to Förster's energy transfer theory [31, 32]. The efficiency of energy transfer, E, is calculated using the equation:

$$E=1-\frac{F}{F_0}=\frac{R_0^6}{R_0^6+r^6} \tag{6}$$

where r is the distance between the donor and acceptor, R_0 is the critical distance when the efficiency of transfer is 50% and can be calculated by the following equation:

$$R_0^6=8.79\times10^{-25}K^2n^{-4}\phi J \tag{7}$$

In Eq. 6, K^2 is the space factor of orientation, n is the refracted index of medium, ϕ is the fluorescence quantum yield of the donor, and J is the effect of the spectral overlap between the emission spectrum of the donor and the absorption spectrum of the acceptor (Fig. 6), which could be calculated by the equation:

$$J=\frac{\int_0^\infty F(\lambda)\varepsilon(\lambda)\lambda^4 d\lambda}{\int_0^\infty F(\lambda)d\lambda} \tag{8}$$

where $F(\lambda)$ is the fluorescence intensity of the donor at wavelength range λ; and $\varepsilon(\lambda)$ is the molar absorption coefficient of the acceptor at λ.

In the present case, K^2=2/3, n=1.36 and ϕ=0.15 [33]. According to the Eqs. 6 to 8, we could calculate that J=7.48×10^{-15} cm^3 1 mol^{-1}, R_0=3.60 nm, E=0.24 and r=4.33 nm. Obviously, the donor-to-acceptor distance r is less than 8 nm, which indicated that the energy transfer from BSA to PAAB occurred with high possibility [34]. It also suggested that the binding of PAAB to BSA was through energy transfer, which was also accord with a static quenching mechanism.

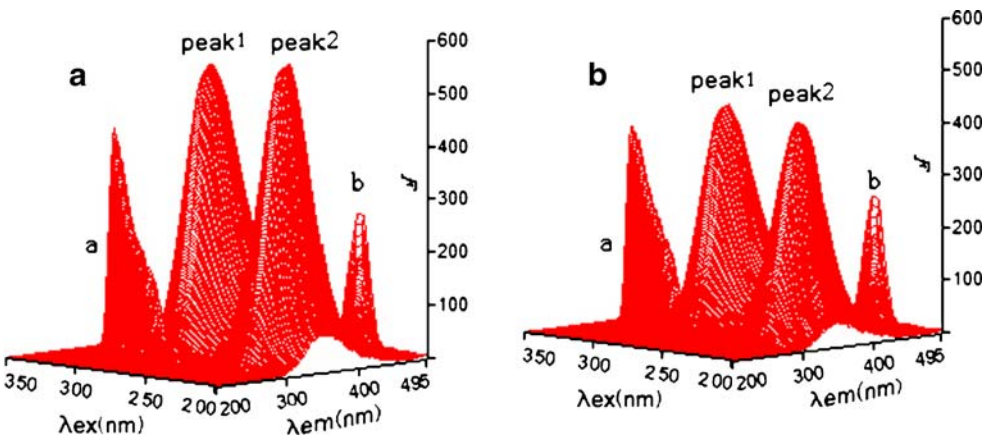

Fig. 9 **a** Three-dimensional fluorescence spectra of BSA, c (BSA)=2.0×10^{-6} mol l^{-1}; and **b** PAAB-BSA complex, c(PAAB)=c(BSA)=2.0×10^{-6} mol l^{-1}

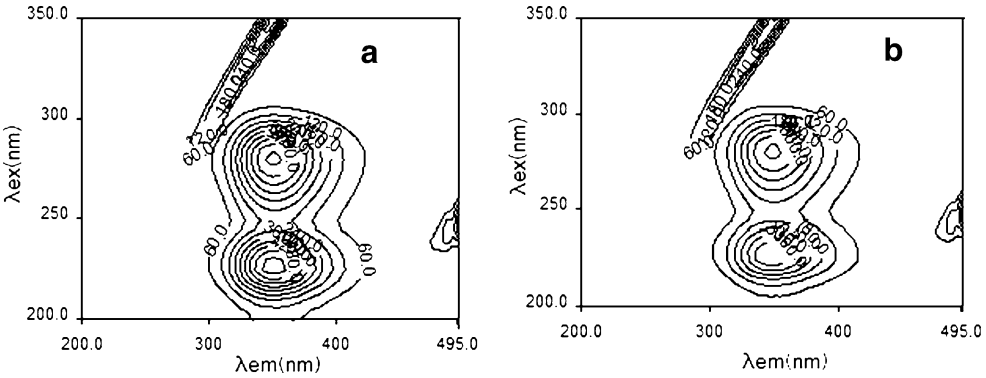

Fig. 10 **a** Contour spectra of BSA, c(BSA)=2.0×10^{-6}mol l^{-1} and **b** PAAB-BSA complex, c(PAAB)=c(BSA)=2.0×10^{-6} mol l^{-1}

Conformational investigation

Synchronous fluorescence spectroscopy

Synchronous fluorescence spectroscopy can give information about the molecular environment in the vicinity of the chromosphere molecules in low concentration under physiological condition. When the D-value ($\Delta\lambda$) between excitation and emission wavelength are stabilized at 15 or 60 nm, the synchronous fluorescence gives the characteristic information of tyrosine or tryptophan residues [35]. It is apparent from Fig. 7a that when $\Delta\lambda$ was set at 15 nm, the maximum emission wavelength blue-shifts 6 nm (from 296 to 290 nm) at the investigated concentrations range; and when $\Delta\lambda$=60 nm (Fig. 7b), the maximum emission wavelength undergoes a slight blue-shift of 3 nm (from 285.5 to 282.5 nm). The blue-shift effect indicated that the microenvironments around tryptophan and tyrosine residues were disturbed and the hydrophobicity of both residues increased in the presence of PAAB.

Circular dichroism spectra

To obtain an insight into the secondary structure of BSA molecules, CD experiments at pH 7.40 and room temperature were carried out. The 1:2, 1:6 and 1:10 molar ratios of BSA to PAAB were used and the CD spectra of BSA in the absence (curve A) and presence (curves B–D) of PAAB were shown in Fig. 8. There are two negative bands in the UV region at 208 and 222 nm, which is the characteristic of α-helical structure of protein [36]. The reasonable explanation is that the negative peaks between 208 and 222 nm are both contributed to $n\rightarrow\pi^*$ transfer for the peptide bond of α-helix [37]. And with the addition of PAAB, the band intensity of curves B to D decreased regularly in the CD spectrum (Fig. 8 curves B–D). The CD results were expressed in terms of mean residue ellipticity (MRE) in degree cm^2 dmol^{-1} according to the following equation [38]:

$$\mathrm{MRE} = \frac{\mathrm{ObservedCD(medg)}}{C_{\mathrm{p}} nl \times 10} \tag{9}$$

where C_{P} is the molar concentration of the protein, n is the number of amino acid residues and l is the path length. The α-helix contents of BSA were calculated from MRE values at 208 nm using the following equation [39]:

$$\alpha - \mathrm{Helical}(\%) = \frac{-\mathrm{MRE}_{208} - 4,000}{33,000 - 4,000} \times 100 \tag{10}$$

where MRE_{208} is the observed MRE value at 208 nm, 4,000 is the MRE of the β-form and random coil conformation cross at 208 nm, and 33,000 is the MRE value of a pure α-helix at 208 nm.

According to the above equations, the percentages of α-helix content of BSA were calculated and shown in Fig. 8. They decreased from 63.57% in free BSA to 51.83% when the molar ratio of PAAB to BSA reached 10:1. The decrease of α-helix content indicated that PAAB combined with the amino acid residues of the main polypeptide chain of protein and destroyed their hydrogen bond networks [4]. Clearly, the addition of PAAB to BSA led to a significant intensity decrease for both negative bands, while the shape

Table 4 Three-dimensional fluorescence spectral characteristics of BSA and PAAB-BSA system

Peaks	BSA			PAAB-BSA		
	Peak position $\lambda_{ex}/\lambda_{em}$ (nm/nm)	Storkes $\Delta\lambda$ (nm)	Intensity F	Peak position $\lambda_{ex}/\lambda_{em}$ (nm/nm)	Storkes $\Delta\lambda$ (nm)	Intensity F
Rayleigh scattering peaks	270/270→350/350	0	29.2→403.4	280/280→350/350	0	29.8→382.5
Fluorescence peak 1	280.0/351.5	71.5	551.1	280.0/348.0	68.0	431.8
Fluorescence peak 2	225.0/352.0	127	571.1	230.0/347.5	117.5	415.2

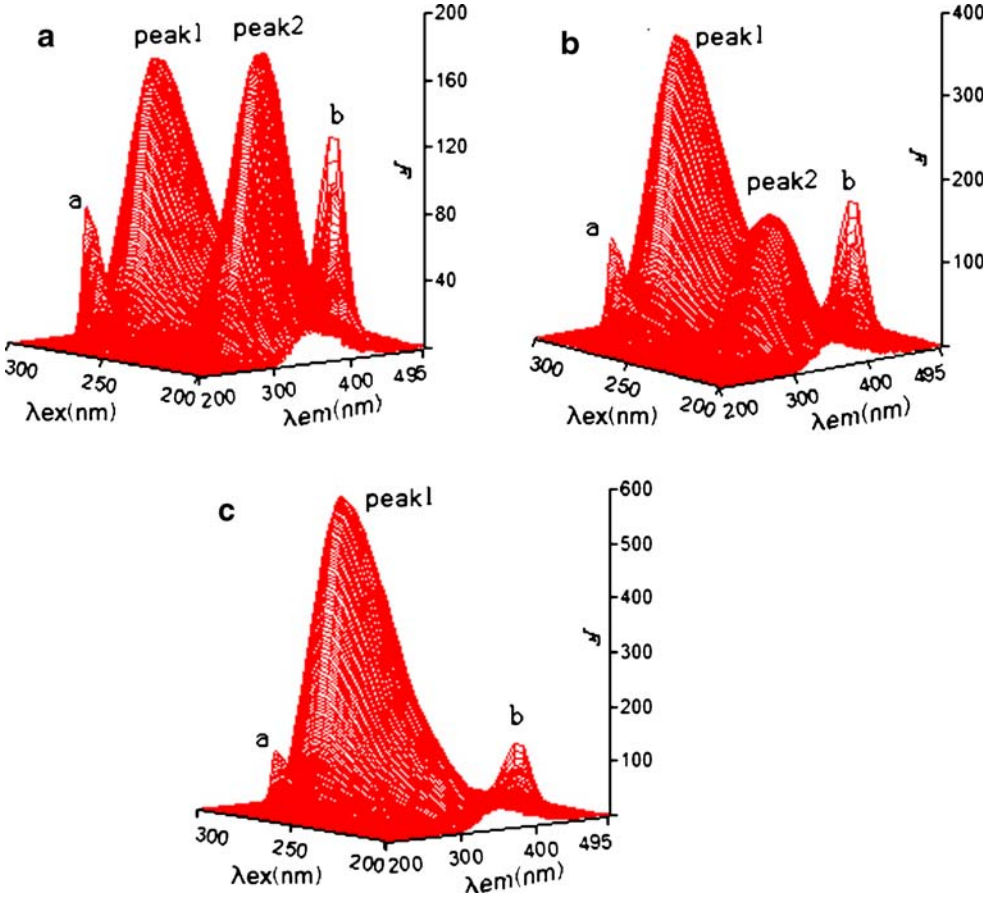

Fig. 11 The three-dimensional fluorescence spectra of BSA at three different concentrations. **a** c(BSA)=2.0×10^{-6} mol l^{-1}; **b** c(BSA)=5.0×10^{-6} mol l^{-1}; **c** c(BSA)=1.0×10^{-5} mol l^{-1} The width of the excitation and emission slit was set to 15.0 and 2.5 nm, respectively

of the peaks and the maximum peak position almost kept the same. It indicated that the binding of PAAB to BSA induced some conformational changes in BSA, while the second structure of BSA was also predominantly of α-helix.

Three-dimensional fluorescence spectra

Additional evidence regarding the conformational changes of BSA in the presence of PAAB came from the three-dimensional fluorescence spectra results and the contour ones. In Figs. 9 and 10, peak *a* is the Rayleigh scattering peak ($\lambda_{ex}=\lambda_{em}$), peak *b* is the second-ordered scattering peak ($\lambda_{em}=2\lambda_{ex}$). Peak 1 which mainly reveals the spectral behavior of tryptophan and tyrosine residues is the primary fluorescence peak we studied, and the maximum emission wavelength and the fluorescence intensity of the residues are in close correlation of their microenvironment's polarity. As can be seen from Fig. 9 and Table 4 that after the addition of PAAB the maximum emission wavelength had a slight blue shift and in the absence and presence of PAAB the fluorescence intensity ratio of peak 1 was 1.28:1. This suggested a less polar environment of both residues and this was consistent with the results of synchronous fluorescence spectra. Bovine serum albumin (BSA) is divided into three linearly arranged and structurally distinct domains (I–III), each domain is composed of two sub-domains (A and B) [40–42], and almost all the hydrophobic

Table 5 The characteristic parameters of three dimensional fluorescence spectra and the α-helix content at different concentrations of BSA

c(BSA) (mol L^{-1})	Fluorescence peak 1		Fluorescence peak 2		α-helix (%)
	Peak position $\lambda_{ex}/\lambda_{em}$(nm/nm)	Intensity F	Peak position $\lambda_{ex}/\lambda_{em}$(nm/nm)	Intensity F	
2.0×10^{-6}	280.0/350.0	189.0	225.0/350.0	207.7	63.57
5.0×10^{-6}	285.0/350.0	347.9	225.0/350.0	139.3	60.03
1.0×10^{-5}	285.0/350.5	560.1	/	/	57.71

amino acid residues are buried in the hydrophobic cavities. So we speculated that the binding position of PAAB to BSA may locate within this hydrophobic pocket, the addition of PAAB changed the polarity of this hydrophobic microenvironment and thus resulting in the conformational changes of BSA.

Moreover, besides peak 1, there is another new strong fluorescence peak (peak 2, λ_{ex}=225.0 nm, λ_{em}=351.5 nm) and the property of this new peak is unclear in the previous studies by others. So we intended to carry out some experiments to investigate the property of this peak. The excitation wavelength of this peak was 225.0 nm, which can provide some clues for us. Comparing with the UV-vis absorption spectra of BSA (Fig. 4, curve B), there is a strong absorption peak at around 230 nm and this peak is mainly caused by the transition of $P \rightarrow P^*$ of BSA's characteristic polypeptide backbone structure C=O; and in the CD spectra (Fig. 8), the negative peaks between 208 and 222 nm are both contributed to $n \rightarrow \pi^*$ transfer for the peptide bond of α-helix [37]. So we speculate that peak 2 may mainly exhibit the fluorescence characteristic of polypeptide backbone structures. In order to confirm this, we studied the three-dimensional fluorescence spectra of BSA at different concentrations (Fig. 11). The characteristic spectral parameters at corresponding concentration (the concentration used were 2.0×10^{-6} mol l^{-1}, 5.0×10^{-6} mol l^{-1} and 1.0×10^{-5} mol l^{-1}) were shown in Table 5. An interesting new phenomenon can be observed that with the increasing concentration of BSA, the fluorescence intensity of peak 1 increased, while the fluorescence intensity of peak 2 decreased obviously. And when the concentration of BSA reached 1.0×10^{-5} mol l^{-1}, peak 2 almost disappeared. The corresponding α-helix content of BSA calculated from the CD experiments was also decreased with the increasing concentration of BSA (Table 5). It may be the result of the interaction of those peptide bonds themselves that decreased the α-helix content and quenched the intrinsic fluorescence of BSA molecules at excitation wavelength of 225.0 nm. This confirmed our speculation that peak 2 may mainly exhibit the fluorescence characteristic of polypeptide backbone structures.

In Fig. 9, the fluorescence intensity of peak 2 decreased a lot after the addition of PAAB (in the absence and presence of PAAB the fluorescence intensity ratio is 1.38:1), which demonstrated that the peptide strands structure of protein was changed and this was in accordance of the decrease of α-helix in the CD spectra. The decrease of the fluorescence intensity of peak 2 in combination with the fluorescence quenching and CD spectra results, we can conclude that the interaction of PAAB with BSA induced the slight unfolding of the polypeptides of protein, which resulted in a conformational change of the protein that increased the exposure of some hydrophobic regions which were previously buried [43]. All these phenomenon and analyzing of peak 1 and peak 2 revealed that the binding of PAAB to BSA induced some microenvironment and conformational changes in BSA.

Conclusions

In this paper, the interaction of PAAB and BSA was investigated mainly by fluorescence quenching spectra, UV–vis absorption spectra, CD and three-dimensional fluorescence spectra. The Stern-Volmer quenching constant K_{SV} and corresponding thermodynamic parameters ΔH, ΔG and ΔS were calculated. The negative values of enthalpy change (ΔH) and entropy change (ΔS) indicated that hydrogen bonds and van der Waals interactions played major roles in stabilizing the complex. The distance r between the donor (BSA) and acceptor (PAAB) was calculated to be 4.33 nm according to Förster's energy transfer theory. The microenvironment and conformation of BSA was demonstrated to be changed in the presence of PAAB by synchronous fluorescence spectra, CD and three-dimensional fluorescence spectra. Moreover, the property of a new fluorescence peak appeared in the three-dimensional fluorescence spectra was proposed and we found the intrinsic fluorescence of BSA might also be quenched by the interaction of polypeptide bond themselves. All these experimental results and theoretical data revealed that PAAB could bind to BSA and be effectively transported and eliminated in body, which could be a useful guideline for further toxicology investigation.

Acknowledgements We gratefully acknowledge the financial support of National Natural Science Foundation of China (Grant no. 30570015, 20621502); Natural Science Foundation of Hubei Province (2005ABC002); Research Foundation of Chinese Ministry of Education ([2006]8-IRT0543); and Chinese 863 program (2007AA06Z407).

References

1. Carter DC, Ho JX (1994) The structure of serum albumin. Adv Prot Chem 45:153–203
2. Zsila F, Bikadi Z, Simonyi M (2003) Probing the binding of the flavonoid quercetin to human serum albumin by circular dichroism, electronic absorption spectroscopy and molecular modelling methods. Biochem Pharmacol 65:447–456
3. Chatterjee S, Srivastava TS (2000) Spectral investigations of the interaction of some porphyrins with bovine serum albumin. J Porphyr Phthalocya 4:147–157
4. Hu YJ, Liu Y, Wang JB et al (2004) Study of the interaction between monoammonium glycyrrhizinate and bovine serum albumin. J Pharm Biomed Anal 36:915–919
5. Hu YJ, Liu Y, Shen XS et al (2005) Studies on the interaction between 1-hexylcarbamoyl-5-fluorouracil and bovine serum albumin. J Mol Struct 738:143–147

6. Wang YQ, Zhang HM, Zhang GC et al (2007) Spectroscopic studies on the interaction between silicotungstic acid and bovine serum albumin. J Pharm Biomed Anal 43:1869–1875
7. Guharay J, Sengupta B, Sengupta PK (2001) Protein-flavonol interaction: fluorescence spectroscopic study. Proteins 43:75–81
8. Zolese G, Falcioni G, Bertoli E et al (2000) Steady-state and time resolved fluorescence of albumins interacting with N-oleylethanolamine, a component of the endogenous N-acylethanolamines. Proteins 40:39–48
9. Gelamo EL, Tabak M (2000) Spectroscopic studies on the interaction of bovine (BSA) and human (HSA) serum albumins with ionic surfactants. Spectrochim Acta Pt A-Mol Bio 56:2255–2271
10. Zollinger H (1991) Color chemistry: synthesis, properties, and applications of organic. Dye. Pigment. 2nd edn. VCH, Weinheim
11. Dirksen A, Zuidema E, Williams RM, De Cola L (2002) Photoactivity and pH sensitivity of methyl orange functionalized poly (Propyleneamine) dendrimers. Macromolecules 35:2743–2747
12. Wang XG, Kumar J, Tripathy SK et al (1997) Epoxy-based nonlinear optical polymers from post azo coupling reaction. Macromolecules 30:219–225
13. Ikeda T, Tsutsumi O (1995) Optical switching and image storage by means of azobenzene liquid-crystal films. Science 268:1873–1875
14. Hugel T, Holland NB, Cattani A et al (2002) Single molecul optomechanical cycle. Science 296:1103–1106
15. Kragh-Hansen U (1981) Molecular aspects of ligand binding to serum albumin. Pharmacol Rev 33:17–53
16. Bhattacharyya M, Chaudhuri U, Poddar RK (1990) Evidence for cooperative binding of CPZ with hemoglobin. Biochem Biophys Res Commun 167:1146–1153
17. Sulkowska A (2002) Interaction of drugs with bovine serum and human serum albumin. J Mol Struct 614:227–232
18. Zhang HX, Huang X, Mei P et al (2006) Studies on the interaction of tricyclazole with â-cyclodextrin and human serum albumin by spectroscopy. J Fluorescence 16:287–294
19. Gelamo EL, Silva CHTP, Imasato H, Tabak M (2002) Interaction of bovine and human serum albumins with ionic surfactants: spectroscopy and modeling. Biochim Biophys Acta 1594:84–99
20. Kang J, Liu Y, Xie MX et al (2004) Interactions of human serum albumin with chlorogenic acid and ferulic acid. Biochim Biophys Acta 1674:205–214
21. Eftink MR (1991) Fluorescence quenching reactions: probing biological macromolecular structures. In: Dewey TG (ed) Biophysical and biochemical aspects of fluorescence spectroscopy. Plenum, New York
22. Lakowica JR, Weber G (1973) Quenching of fluorescence by oxygen, a probe for structural fluctuations in macromolecules. Biochemistry 12:4161–4170
23. Maurice RE, Camillo AG (1981) Fluorescence quenching studies with proteins. Anal Biochem 114:199–212
24. Ware WR (1962) Oxygen quenching of fluorescence in solution, an experimental study of the diffusion process. J Phys Chem 66:455–458
25. Papadopoulou A, Green RJ, Frazier RA (2005) Interaction of flavonoids with bovine serum albumin: a fluorescence quenching study. J Agric Food Chem 53:158–163
26. Lehrer SS (1971) The quenching of the tryptophyl fluorescence of model compounds and of lysozyme by iodide ion. Biochemistry 10:3254–3263
27. Ross PD, Subramanian S (1981) Thermodynamics of protein association reaction: forces contribution to stability. Biochemistry 20:3096–3102
28. Liu JQ, Tian JN, Zhang JY et al (2003) Interaction of magnolol with bovine serum albumin: a fluorescence quenching study. Anal Bioanal Chem 376:864–867
29. Tian JN, Liu JQ, Zhang JY et al (2003) Fluorescence studies on the interactions of barbaloin with bovine serum albumin. Chem Pharm Bull 51:579–582
30. Jiang M, Xie MX, Zheng D et al (2004) Spectroscopic studies on the interaction of cinnamic acid and its hydroxyl derivatives with human serum albumin. J Mol Struct 692:71–80
31. Sklar LA, Hudson BS, Simoni RD (1977) Conjugated polyene fatty acids as fluorescent probes: binding to bovine serum albumin. Biochemistry 16:5100–5108
32. Cui FL, Fan J, Li JP, Hu ZD (2004) Interactions between 1-benzoyl-4-pchloro-phenyl thiosemicarbazide and serum albumin: investigation by fluorescence spectroscopy. Bioorg Med Chem 12:151–157
33. Cyril L, Earl JK, Sperry WM (1961) In: Biochemists' handbook, E & FN Spon, London, pp 84.
34. Bi S, Song D, Tian Y et al (2005) Molecular spectroscopic study on the interaction of tetracyclines with serum albumins. Spectrochim Acta Pt A-Mol Bio 61:629–636
35. Miller JN (1979) Recent advances in molecular luminescence analysis. Proc Anal Div Chem Soc 16:203–208
36. Liu JQ, Tian JN, Tian X et al (2004) Interaction of isofraxidin with human serum albumin. Bioorg Med Chem 12:469–474
37. Yang P, Gao F (2002) The principle of bioinorganic chemistry. Science Press, p 349
38. Li Y, He W, Liu J et al (2005) Binding of the bioactive component jatrorrhizine to human serum albumin. Biochim Biophys Acta 1722:15–21
39. Lu ZX, Cui T, Shi QL (1987) In molecular biology, applications of circular dichroism and optical rotatory dispersion, 1st ed. Science Press, pp79–82
40. Brown KF, Crooks MJ (1976) Displacement of tolbutamide, glibencalmide and chlorpropamide from serum albumin by anionic drugs. Biochem Pharmacol 25:1175–1178
41. Rosenoer VM, Oratz M, Rothschild MA (eds) (1977) In: Albumin structure, *function and uses*. Pergamon, New York, pp 113–141
42. Peters T (1995). In: All about albumin: biochemistry, genetics and medical applications. Academic, San Diego, CA, Chapter 6, pp 251–284
43. Tian JN, Liu JQ, Hu ZD, Chen XG (2005) Interaction of wogonin with bovine serum albumin. Bioorg Med Chem 13:4124–4129